Dynamic Localization Phenomena in Elasticity, Acoustics and Electromagnetism

CISM International Centre for Mechanical Sciences Volume 547, 2013, pp 181-223

Trapped Modes and Edge Resonances in Acoustics and Elasticity

Vincent Pagneux

Laboratoire d'Acoustique de l'Université du Maine, LAUM UMR CNRS 6613, Le Mans, France

Abstract This chapter considers localized modes for acoustic and elastic waves. We first discuss trapped modes for acoustic scalar waves that are perfectly localized solutions near defects in waveguides with a real resonance frequency. Emphasis is given on the trapping mechanism coming from the evanescent nature of transverse modes in waveguides. We then study the case of quasi-trapped modes where the wave is strongly localized but can radiate energy. Complex resonance frequencies are shown to appear through approximate models and general principles. Eventually, we focus on elastic wave localization near traction free edges in plates and rods. The complicated polarization of the wave in elasticity is shown to increase the ability for trapping with very simple geometries.

1 Introduction

Modes are solutions of the wave equation without sources. They provide a very powerful tool to understand the response of wave systems when excited by a source because they represent an intrinsic basis corresponding to various kind of resonances. When the frequency is close to a resonance frequency the solution is dominantly given by the corresponding mode. The more often, modes are defined for closed cavity where the boundaries are able to quantify the frequencies. Here, we are concerned with trapped modes and localized solutions that exist for open geometry with confinement in at least one direction. These waveguide structures support evanescent waves that facilitate the trapping. Trapped modes were introduced more than fifty years ago (see for instance Jones (1953)) and since then have induced an important amount of works (Callan et al., 1991; Evans et al., 1994; Kaplunov and Sorokin, 1995; Granot, 2002; Bonnet-BenDhia and Mercier, 2007). Recent comprehensive reviews can be found in Linton and McIver (2007) and Postnova and Craster (2008).

In these notes, in section 2, a reminder on the usual modes in a closed cavity is presented, followed by a brief introduction to trapped modes in open geometries. Section 3 is dedicated to trapped modes for scalar waves. The basic mechanism of trapping is illustrated with the simple model of the potential well. Then, the case of waveguides with Dirichlet boundary conditions is dealt with. Acoustic waveguides with Neumann boundary conditions give a more subtle situation where trapping occurs owing to symmetries that allow to localize the solution. Waves localized but radiating energy are discussed in section 4. A simple model permits to introduce the complex resonance frequencies corresponding to these quasi-trapped modes and basic analytical properties in the complex frequency plane are presented. In section 5, we look at elastic waveguides and their particularity. It is shown that the vectorial nature of the elastic waves, with longitudinal and transversal polarizations, offers the ability to trap the solution near traction free edge, either in plates or in rods.

2 Different kinds of modes

In the first four sections of these notes we will consider scalar waves. In the harmonic regime, with the time dependence chosen as $e^{-i\omega t}$, they are governed the Helmholtz equation

$$\triangle\phi + k^2\phi = 0, \tag{1}$$

where $k = \omega/c$. If c does not depend on ω the scalar wave is dispersionless: typically it corresponds to acoustic waves (Morse and Ingard, 1968). If $dc/d\omega \neq 0$ the wave is dispersive as is the case for instance for water waves (Cobelli et al., 2011). The Helmholtz equation (1) has to be supplemented by boundary conditions. The more often[1] they are of the Dirichlet or Neumann type: $\phi = 0$ at the wall for Dirichlet and $\partial_n\phi = 0$ for Neumann. Depending on the physical problem, Dirichlet or Neumann boundary conditions (BC) are applied as summarized below:

- Acoustics (Neumann BC at hard wall)
- Electromagnetism 2D (Neumann or Dirichlet BC for perfect metal)
- Elasticity with SH polarization (Neumann BC for stress free interface)
- Quantum mechanics (Dirichlet BC at hard wall)
- Water waves (Neumann BC at vertical hard wall)

In all these cases we have to deal with a scalar wave represented by a single scalar function ϕ. In the following, a heuristic introduction to the notion

[1] Note that mixed boundary conditions exist also: they correspond to a local impedance or a local admittance.

of modes for the usual case of a closed cavity and the unusual case of open geometry is given.

2.1 Modes in cavity (usual)

The usual modes are solutions of the homogeneous Helmholtz equation (1) in a closed cavity. Figure 1 displays the example of a mode in an acoustic cavity with hard wall. The wave cannot escape the cavity and the boundary conditions are able to select a particular set of discrete frequencies k_n and eigenmodes ϕ_n that satisfy

$$\triangle\phi_n + k_n^2\phi_n = 0, \tag{2}$$

with $\partial_n\phi_n = 0$ on the boundary, and where n is the index of the mode. The

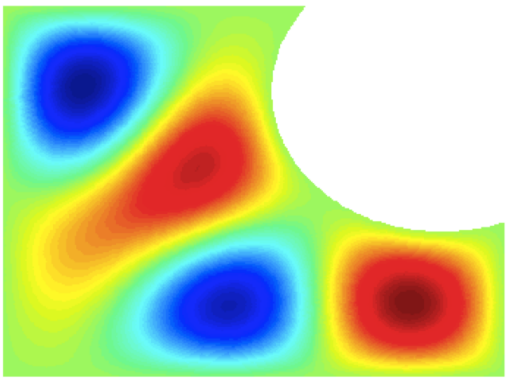

Figure 1. A mode in an acoustic cavity.

set of modes ϕ_n provides an orthonormal basis[2] with the property:

$$(\phi_m|\phi_n) = \delta_{nm}, \tag{3}$$

where the scalar product is defined as $(\phi|\psi) = \int \overline{\phi(\boldsymbol{x})}\psi(\boldsymbol{x})d\boldsymbol{x}$. The usefulness of the modes can now be illustrated when we want to solve the wave equation in the same cavity with a source s:

$$\triangle\phi + k^2\phi = s(\boldsymbol{x}). \tag{4}$$

[2]It comes from the self-adjointness of the problem, for details on the mathematical aspects see for instance Stakgold (1998).

The sought ϕ can be expanded on the mode basis as

$$\phi(\boldsymbol{x}) = \sum_n c_n \phi_n(\boldsymbol{x}). \tag{5}$$

Inserting this expansion in the wave equation and using the orthonormality (3), the coefficients c_n are found to be

$$c_n = \frac{(s|\phi_n)}{k^2 - k_n^2}. \tag{6}$$

When $k \simeq k_n$, the solution is dominantly given[3] by the mode ϕ_n. We see here the intrinsic character of the modes: they provide a set of functions independent of sources and they govern the wave with source when the imposed frequency is close to a resonance frequency.

2.2 Modes in open geometry (unusual)

We have seen that a closed cavity sustains an infinite of modes. In open geometry the wave has the ability to radiate towards infinity so that in general there is no homogeneous solution of the Helmholtz equation with finite energy. Nevertheless, for open geometry where the wave can be evanescent towards infinity, we will see that it is possible to obtain trapped mode. A

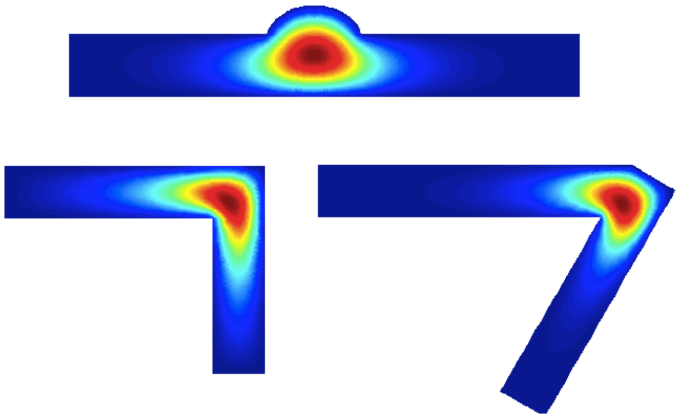

Figure 2. Trapped modes in three different waveguides with Dirichlet boundary conditions. (top) bump, (bottom) bends.

[3] Assuming that the projection of the source term $(s|\phi_n)$ is not zero.

trapped mode is defined as an homogeneous solution of the wave equation ($\triangle\phi + k^2\phi = 0$) with finite energy,

$$\int |\phi|^2 d\boldsymbol{x} \text{ finite.}$$

It is associated with a real resonance frequency k and the set of resonance frequencies of trapped modes for a given geometry is discrete. Waveguides are the typical geometries where trapped modes may exist because in such geometries the wave propagates towards infinity through a finite number of propagating transverse modes and an infinite number of evanescent waves. For instance, for waveguides with Dirichlet boundary conditions, there is a frequency threshold below which the wave is purely evanescent in the leads towards infinity. Below this threshold, the wave cannot escape from a defect in the waveguide and a trapped mode can be easily found. Figure 2

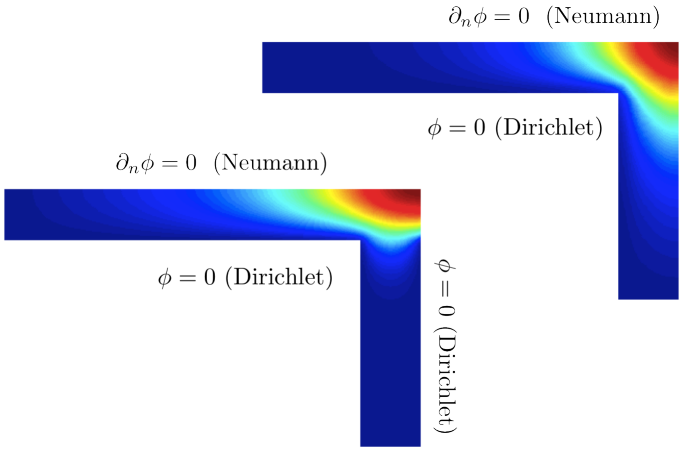

Figure 3. Trapped modes in bent waveguides with a mixing of Dirichlet and Neumann boundary conditions in the leads.

shows three examples of trapped mode for waveguides with Dirichlet boundary conditions[4]. Boundary conditions of different types can also support trapped modes. Figure 3 correspond to trapped modes in bent waveguides with a mixing of Dirichlet and Neumann boundary conditions. The trapping is still rather "easy" since a waveguide with Neumann BC on one side

[4]This situation is common in quantum mechanics where these modes are called bound states.

and Dirichlet BC on the other side still has a non-zero frequency threshold where the wave cannot propagate. The case of waveguides with Neumann boundary conditions (as in acoustics) needs a little more of subtlety. The plane is always propagating with no cut-on frequencies and the wave is able to radiate towards infinity even for low frequencies. Nevertheless, as will be described with more details in the next section, by using symmetry of the geometry it is possible to recover the same situation as for Dirichlet waveguides where the antisymmetric part of the wave is evanescent below a threshold frequency. Examples of trapped modes for symmetric acoustic waveguides are shown in Figure 4.

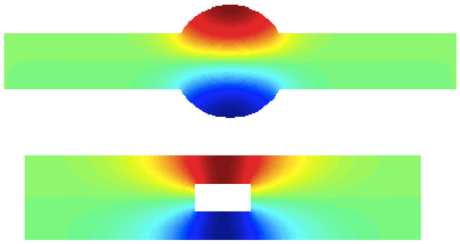

Figure 4. Trapped modes for symmetric waveguides with Neumann boundary conditions (acoustic case).

3 Trapped modes for scalar waves

Trapped modes can exist in waveguides, i.e. system confined in at least one direction, where evanescent waves are able to localize the energy around a defect. The basic mechanism of trapping is well described by the simple model of the potential well.

3.1 Trapping mechanism: the potential well

The potential well is illustrated in Figure 5. In this model, the wave is governed by the Schrodinger equation

$$\phi'' + (k^2 - V(x))\phi = 0, \tag{7}$$

where V is the potential (further details on the physical context can be found for instance in Landau and Lifshitz (1977)). For this model, V is constant ($V = V_0$) except in a the central region $|x| < a$ where it is zero (see Fig. 5). The equations inside the well and outside the well are respectively

$$|x| < a : \quad \phi'' + k^2\phi = 0 \tag{8}$$

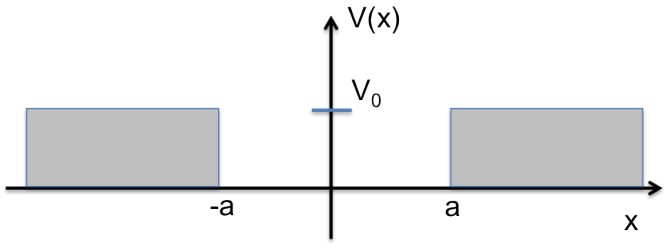

Figure 5. The potential well.

and

$$|x| > a : \quad \phi" + (k^2 - V_0)\phi = 0. \tag{9}$$

Inside the well, for $|x| < a$, the wave can always propagate, but the propagation of the wave outside the well, for $|x| > a$, is controlled by the sign of $k^2 - V_0$. If $k^2 < V_0$, the wave is evanescent and the it will be seen that a trapped mode exists.

Trapping case: $k^2 < V_0$. In this case, the wave is evanescent outside the well. A trapped mode is a solution of the homogeneous wave equation (7) with outgoing radiation condition outside the well. Benefiting from the symmetry of the problem with respect to $x = 0$, we are looking for a trapped mode even in x. Inside the well, $|x| < a$, the solution is

$$\phi = A \cos kx \tag{10}$$

and for $|x| > a$ the outgoing radiation condition selects a solution of the form

$$\phi = Be^{-\alpha|x|}. \tag{11}$$

The continuity of ϕ and ϕ' at $x = a$ yields an implicit equation on k:

$$k \tan ka = \alpha, \tag{12}$$

where $\alpha = \sqrt{V_0 - k^2}$. This implicit equation can solved graphically as shown in Figure 6. Whatever the value of V_0, it is obvious that it posses at least one solution k_R that corresponds to the resonance frequency of a trapped mode. When V_0 goes to zero, it is possible to obtain an approximate explicit resonance frequency:

$$k_R^2 \simeq V_0 - V_0^2 a^2.$$

It is typical of a trapped mode with a weak defect: the resonance frequency is asymptotically close to (and below) the threshold (or the cut-on frequency,

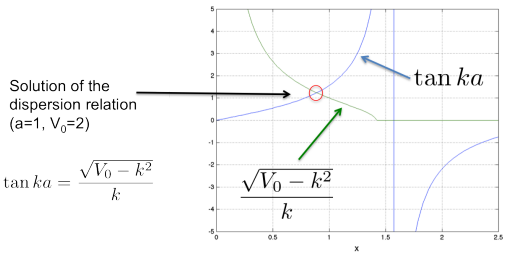

Figure 6. Resolution of the implicit equation of the trapped mode.

here represented by $\sqrt{V_0}$) where the wave becomes propagative. This kind of results are also found for trapped in waveguides with small defect (Nazarov, 2011). The shape of the trapped mode calculated for $a = 1$ and $V_0 = 2$ is shown in Figure 7. The corresponding resonance frequency solution of the implicit equation (12) is numerically found to be $k_R = 0.89$. The

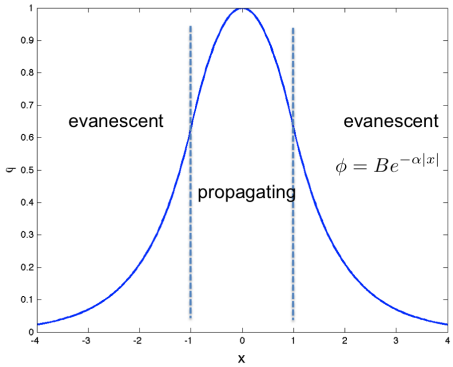

Figure 7. Shape of the trapped mode for $a = 1$ and $V_0 = 2$. The resonance frequency is $k_R = 0.89$.

structure of trapping appears. Inside the well, playing the role of a defect, the wave is propagating and it cannot radiate towards infinity since the wave is evanescent outside. Actually, we have the same situation as in a closed cavity with the evanescent region playing the role of effective walls.

Scattering case: $k^2 > V_0$. When the frequency is above the threshold ($k^2 > V_0$) the wave is propagating everywhere. The trapping is not possible and the solution to the wave equation is in the form of a scattering state (Landau and Lifshitz, 1977). For $x < -a$

$$\phi = e^{i\beta x} + Re^{-i\beta x}, \tag{13}$$

and for $x > a$

$$\phi = Te^{i\beta x}, \tag{14}$$

where $\beta = \sqrt{k^2 - V_0}$. The scattering coefficients can be found (Landau and Lifshitz, 1977) from the linear system of four equations with four unknowns obtained by applying the continuity of ϕ and ϕ' at $x = \pm a$ with the solution inside the well ($|x| < a$) given by

$$\phi = A\cos kx + B\sin kx. \tag{15}$$

It appears that no trapping is possible in this case because as soon as

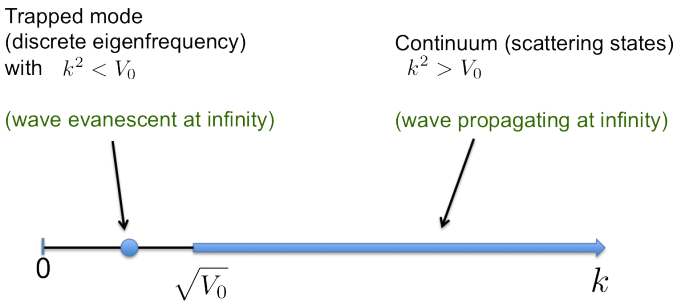

Figure 8. Spectrum of the potential well.

the wave is nonzero it has to radiate energy towards infinity. A sketch of the spectrum along the frequency axis k is shown in Figure 8. Above the threshold, we have the scattering states for the continuous set of k such that $k > \sqrt{V_0}$. Below the threshold, no wave can propagate towards infinity and the trapping is possible for some discrete values of k. These resonance frequencies are selected by interference effect in the propagating well with the effective wall effects of the evanescence regions. In this particular model of the potential well there is at least one trapped mode, but in other situations with a similar threshold frequency it is possible that no trapping occurs (Nazarov, 2011).

The simple mechanism of trapping that has been described is the typical one in other wave system for open geometries in 1D, 2D and 3D. The

important property is the existence of a frequency gap for which the wave is evanescent towards infinity. Then, for frequencies inside the gap, the evanescence environment is able to play the role of an effective wall for a defect and we recover the situation of a closed cavity. In the following, we focus on waveguides in 2D that naturally present cut-on frequencies creating the frequency gap.

3.2 Dirichlet waveguide

Trapped modes are solutions of the homogeneous wave equation with outgoing radiation conditions. We have seen that evanescence is the way to be trapped and the perfect candidates are thus waveguide geometries. We begin with Dirichlet waveguides where previously discussed frequency gap appears more simply than for Neumann waveguides. The transverse modes

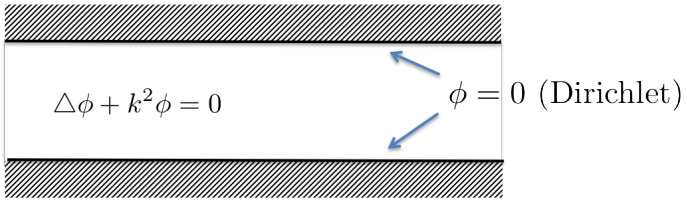

Figure 9. Dirichlet waveguide of width h.

of the waveguide are necessary to make to appear the evanescent character of the propagation. They are defined as solution of the wave equation in a straight waveguide (Figure 9) sought in the separable form:

$$\phi(x, y) = e^{i\alpha x} g(y). \tag{16}$$

Inserting this form into the wave equation gives the ordinary differential equation on the function g:

$$\frac{d^2 g}{dy^2} + (k^2 - \alpha^2) g = 0. \tag{17}$$

On the other hand, the Dirichlet boundary conditions on the wall, $\phi = 0$ for $y = 0 = h$, implies that

$$g(0) = g(h) = 0. \tag{18}$$

Equations (17) with (18) have an infinite discrete set of solutions

$$g_n(y) = \sqrt{\frac{2}{h}}\ \sin(\frac{n\pi y}{h}) \tag{19}$$

indexed by the integer $n \geq 1$. The pre-factor $\sqrt{2/h}$ is chosen so as to ensure the orthonormality of the transverse modes

$$\int_0^h g_n(y) g_m(y) dy = \delta_{nm}.$$

Each transverse mode is associated to an axial wavenumber α indexed by $n \geq 1$:

$$\alpha_n^2 = k^2 - \left(\frac{n\pi}{h}\right)^2. \tag{20}$$

Here comes the propagating or evanescent waves. For a given frequency k, a transverse mode is either propagating (real α_n) or evanescent (imaginary α_n) depending on the sign of α_n^2. Thus for $k > n\pi/h$ the wave is propagating and for $k < n\pi/h$ the wave is evanescent. Since $n \geq 1$ there appears that all the transverse modes are evanescent for $k < \pi/h$. The

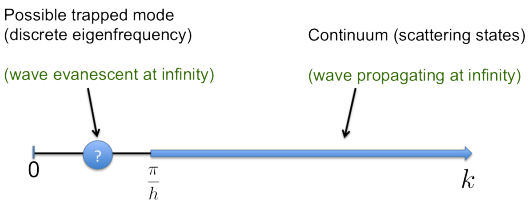

Figure 10. Spectrum of the Dirichlet waveguide with lead width h.

general solution of the wave equation can be expanded[5] on the infinite set of transverse modes[6] as

$$\phi = \sum_0^\infty (c_n e^{i\alpha_n x} + d_n e^{-i\alpha_n x}) g_n(y), \tag{21}$$

which means that for $k < \pi/h$ any wave solution is only composed of evanescent waves. For $k > \pi/h$, at least the mode with $n = 1$ is propagating and when the frequency increases more and more transverse modes are propagating with the cut-on frequencies at $k_{c,n} = n\pi/h$. In the presence of a defect, similarly to the model of the potential well, a sketch of the spectrum along the frequency axis k can be given (Figure 10). For a Dirichlet

[5] The terms $e^{\pm i\alpha_n x}$ correspond respectively to right/left going waves.

[6] These transverse modes play the role of generalized Fourier series modes and form a complete basis on $0 \leq y \leq h$ (Stakgold, 1998).

waveguide, with leads towards infinity of width h, the wave cannot propagate in a gap $0 < k < \pi/h$. Thus a the existence of a trapped mode is possible in this gap, depending of the shape of the defect between the leads. For a local perturbation of the width of the waveguide corresponding to an increase of the volume it can be proven that a trapped mode exists and asymptotic approximations of the resonance frequencies can be obtained (Nazarov, 2011). Figure 11 displays the pattern of such a trapped mode. For the case of bent quantum waveguides, there is an important literature discussing the existence of trapped modes often called bound states in this quantum mechanics community (Duclos and Exner, 1995).

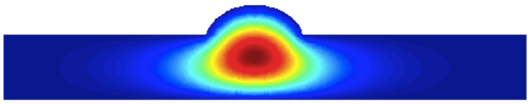

Figure 11. Trapped mode for a defect in Dirichlet waveguide.

3.3 Neumann waveguide

The question of trapped modes in waveguides with Neumann boundary conditions is more involved because the plane transverse mode can always propagate. Indeed, when seeking a separable solution of the form $\phi = e^{i\alpha x}g(y)$ in the geometry shown in Figure 12, the ODE for g is the same as for Dirichlet waveguides,

$$g" + (k^2 - \alpha^2)g = 0, \tag{22}$$

but the Neumann boundary conditions imply that

$$g'(0) = g'(h) = 0. \tag{23}$$

The transverse modes are thus of the form

$$g_n(y) = \sqrt{\frac{2-\delta_0}{h}}\ \cos(\frac{n\pi y}{h}), \tag{24}$$

where $n \geq 0$ and with the pre-factor permitting the orthonormality

$$\int_0^h g_n(y)g_m(y)\ dy = \delta_{nm}.$$

Following the same reasoning as in the previous section, the transverse

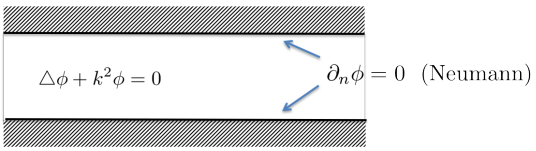

Figure 12. Neumann waveguide of width h.

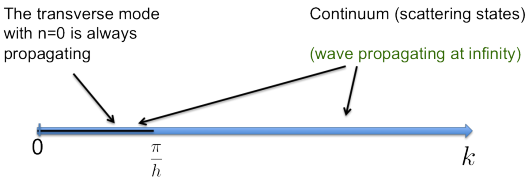

Figure 13. Structure of the spectrum for a Neumann waveguide with lead width h.

mode indexed by n is propagating if $k > n\pi/h$. The novelty here is that the plane transverse mode (with $n = 0$) has no cut-on frequency and can propagate for any frequency. The spectrum is shown in Figure 13.

Thus, the wave can radiate towards infinity whatever the frequency. To create a gap we need to decouple the plane wave mode from the other ones. The "trick" is then to use the symmetry of the geometry in order to get the decoupling. Indeed, for a waveguide symmetric with respect with the axis x (Figure 14), the symmetric part (even w.r.t. y) of the solution ϕ_s and the antisymmetric part (odd w.r.t. y) ϕ_a of the solution are defined as

$$\phi_s(x,y) = \frac{1}{2}\left(\phi(x,y) + \phi(x,-y)\right) \tag{25}$$

and

$$\phi_a(x,y) = \frac{1}{2}\left(\phi(x,y) - \phi(x,-y)\right). \tag{26}$$

These two parts of the wave are decoupled owing to the symmetry of the

Figure 14. A symmetric waveguide.

geometry. Consequently, we have in fact two decoupled problem for wave

propagation in this case: the symmetric part of the wave associated with the even transverse modes indexed by even integers (n=0,2,4,...) and the anti-symmetric part of the wave associated with odd transverse modes indexed by odd integers (n=1,3,5,...). Since the plane mode with $n = 0$ belongs to the first part, the decoupling due to the symmetry allows to recover the same threshold (cut-on frequency) as for the waveguide with Neumann boundary conditions. The gap exists for the antisymmetric part of the wave (Figure 15). The existence of trapped modes for Neumann waveguides using this

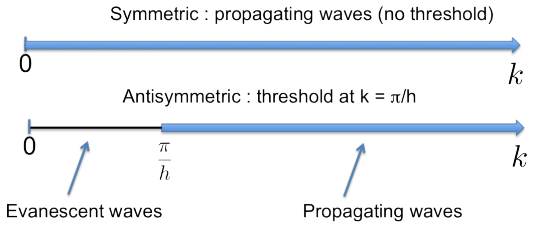

Figure 15. Spectrum for a symmetric waveguide with lead width h.

symmetry argument is the classical one in the literature (Evans et al., 1994). In Figure 16 the example of such a trapped mode is shown for the geometry of an acoustic expansion chamber.

Figure 16. A trapped mode in symmetric Neumann waveguide.

3.4 Approximate mode matching

The determination of trapped modes is difficult and needs usually full numerical computations, but, for some geometries, it is possible to find simple approximations. In the case of a rectangular obstacle (Fig 17), mode matching techniques can be applied and useful simple analytical approximations can be found. Consider the geometry shown in Figure 17: it is symmetric with Neumann boundary conditions and as such can accept a trapped mode solution (remind that it is a solution of the homogeneous

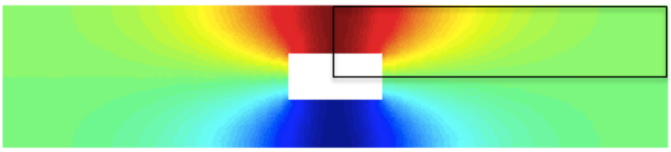

Figure 17. Trapped mode for a symmetric rectangular obstacle in a Neumann waveguide.

Helmholtz equation (1) with outgoing radiation condition). The trapped mode has to be an antisymmetric solution as discussed in the previous section, and by symmetry the domain can be reduced to the rectangle drawn in Figure 17 and reproduced in Figure 18. To apply an approximate mode matching technique we choose to keep just the plane mode in the central region of Figure 18 but to take into account the full set of evanescent waves outside the obstacle. Thus the solution for $0 < x < a$ is approximated by

$$\phi(x, y) = A \cos(kx) \tag{27}$$

and outside the obstacle ($x > a$) the solution is expanded on the full series of evanescent modes,

$$\phi(x, y) = \sum_{n \geq 0} c_n e^{-K_n} g_n(y), \tag{28}$$

where $K_n = \sqrt{\gamma_n^2 - k^2}$, $\gamma_n = (2n + 1)\pi/h$ and $g_n(y) = 2/\sqrt{h} \sin \gamma_n y$. Note that, since we are in the frequency gap $k < \pi/h$ (see previous section), $\gamma_n > k$ for all n. The following interface boundary conditions have to be

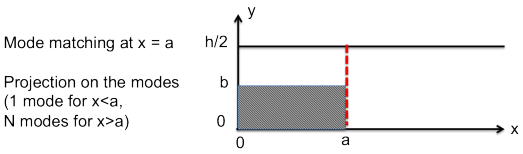

Figure 18. Partition of the problem.

satisfied at $x = a$:

$$\phi(a^+, y) = \phi(a^-, y) \quad \text{for} \quad b < y < h/2 \tag{29}$$

and

$$\partial_x\phi(a^+,y) = \partial_x\phi(a^-,y) \quad \text{for} \quad b < y < h/2, \tag{30}$$

$$\partial_x\phi(a^+,y) = 0 \quad \text{for} \quad 0 < y < b. \tag{31}$$

Mode matching consists in projecting equations (29–31) on the transverse modes that have been taken into account in the solution expansion in (27–28). Projection of the continuity of ϕ on the plane mode,

$$\int_b^{h/2} \phi(a^+,y)\, dy = \int_b^{h/2} \phi(a^-,y)\, dy, \tag{32}$$

yields a first relation between the unknown coefficients A and c_n:

$$\sum_{n\geq 0} c_n \int_b^{h/2} g_n(y)\, dy = A(h/2-b)\cos(ka). \tag{33}$$

On the other hand projection of equations (30-31) on each of the outside transverse modes is done through

$$\int_0^{h/2} \partial_x\phi(a^+,y) g_n(y)\, dy = \int_b^{h/2} \partial_x\phi(a^+,y) g_n(y)\, dy \tag{34}$$

$$= \int_b^{h/2} \partial_x\phi(a^-,y) g_n(y)\, dy, \tag{35}$$

and it gives for each $n \geq 0$:

$$K_n c_n = Ak\sin(ka) \int_b^{h/2} g_n(y)\, dy. \tag{36}$$

Eventually, by eliminating c_n between (33) and (36), we obtain

$$\tan(ka) = \frac{h}{8}(h-2b) \frac{1}{\displaystyle\sum_{n\geq 0} \frac{\cos(\gamma_n b)}{\gamma_n} \frac{k}{\sqrt{\gamma_n^2 - k^2}}} \tag{37}$$

where k is the unknown. This determines implicitly the resonance frequency. The $k = k_R$ solution is a good approximation when the rectangular obstacle is long enough because it neglects the higher order modes for $x < a$.

3.5 Mathematical proof: variational technique

These notes are not really mathematically oriented and the rigorous approach to trapped modes can be found in the functional analysis literature (Duclos and Exner, 1995; A.S. Bonnet-BenDhia and Mahé, 1997; Bonnet-BenDhia and Mercier, 2007; Nazarov, 2011). Nevertheless we briefly present here the popular variational technique often used to prove the existence of trapped mode.

The idea comes from the min-max principle for an hermitian matrix of finite size ($M = \overline{M}^T$). It states that the eigenvalues λ_n of M verify

$$\min(\lambda_n) \leq \frac{(x|Mx)}{(x|x)}$$

$\forall x \neq 0$. We recognize here the Rayleigh quotient. This latter can be also defined for the eigenvalue problem corresponding to trapped mode under the form

$$Q(\psi) = \frac{\int |\nabla\psi|^2 d\mathbf{x}}{\int |\psi|^2 d\mathbf{x}}.$$

Here ψ is a square integrable[7] test function respecting the imposed boundary conditions (i.e. ψ must be in the domain of the operator). Then, the variational min-max principle (Bonnet-BenDhia and Mercier, 2007) states that if

$$Q(\psi_0) < \frac{\pi^2}{h^2}$$

for some test function ψ_0 then there exists a trapped mode with resonance frequency k_R such that

$$k_R \leq \sqrt{Q(\psi_0)}.$$

What is nice here is that it is sufficient to cleverly choose a test function which is not a solution of the wave equation to prove the existence of a trapped mode. Let us take the simple example of the trapped mode for the Neumann waveguide with a rectangular obstacle (Figure 19). We can choose the test function defined by

$$\psi_0 = \text{sign}(y)\cos(\frac{\pi x}{2a})$$

for $|x| < a$ and

$$\psi_0 = 0$$

[7] In the sense that the function and its gradient are square integrable so that the Rayleigh quotient is well defined.

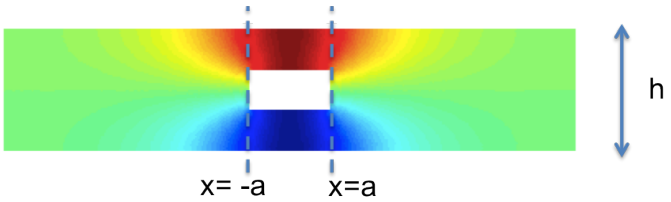

Figure 19. Trapped mode in the Neumann waveguide with rectangular obstacle.

for $|x| > a$.

Of course this test function is not a solution of the Helmholtz equation but it is square integrable (as is its gradient) and it verifies the Neumann boundary condition at the wall. A simple computation shows that

$$Q(\psi_0) = \frac{\int |\nabla \psi_0|^2 d\mathbf{x}}{\int |\psi_0|^2 d\mathbf{x}} = \frac{\pi^2}{4a^2}.$$

From the variational principle min-max principle, we know that a trapped mode exists if

$$Q(\psi_0) = \frac{\pi^2}{4a^2} \leq \frac{\pi^2}{h^2}. \tag{38}$$

Hence, from the variational principle and (38), we can conclude that a

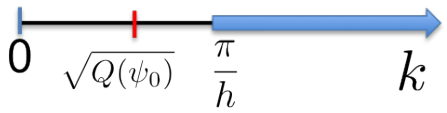

Figure 20. Spectrum of the Neumann waveguide with rectangular obstacle.

trapped mode exists if

$$a > h/2$$

and that the corresponding resonance frequency will satisfy

$$k_R < \frac{\pi}{2a}.$$

The corresponding scheme of the spectrum is shown in Figure 20.

By this example, we see how powerful is this variational technique: with the very simple choice of the test function ψ_0 it has been possible to rigorously prove the existence of the trapped mode and to find an upper bound for the resonance frequency.

3.6 Higher frequencies

So far, we have focused on trapped modes at low frequencies. Their existence can be understood from the existence of a frequency gap $0 < k < \pi/h$ where the waves are evanescent in outgoing leads of the waveguide. For higher frequencies, trapped modes can also exist but their existence is more difficult to show. Heuristically, it can be argued there that for higher cut-on frequencies there exists "gaps" with a finite number of transverse mode that can radiate. A trapped mode has to be in "good interferences" in order to annihilate the component on this finite number of modes. In such a situation, McIver et al. (2001) have chosen the term embedded trapped modes to stress that no symmetry is able to decouple the modes from the continuous spectrum of scattering states[8]. By taking an obstacle with several parameters they have shown that is possible to construct trapped mode above the threshold of evanescence given by symmetries of the geometry.

Figure 21 displays the example of a trapped mode with a resonance frequency above the threshold of evanescence ($k > \pi/h$) for a Dirichlet waveguide. In this case two propagating transverse modes might radiate towards infinity.

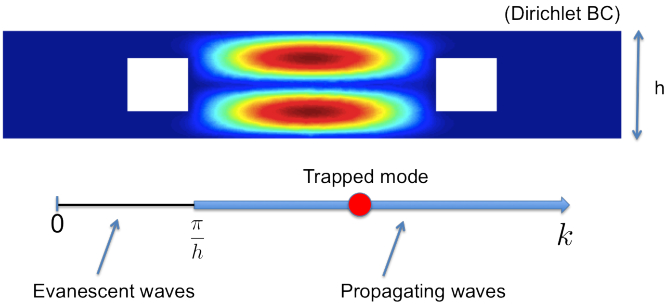

Figure 21. Trapped mode for a Dirichlet waveguide at higher frequencies.

4 Quasi-trapped modes and edge waves

4.1 Quasi-trapped modes and complex resonance

The trapped modes previously discussed are very particular object that are perfectly localized in infinite waveguide. But waves can also be localized

[8] These modes are often called BIC (Bound States in the Continuum) in quantum mechanics.

with a small leakage. This corresponds to quasi-trapped modes (or complex resonance as we shall see).

Figure 22. Localized wave in a thin slot.

As an example, consider the geometry shown in Figure 22: a semi-infinite acoustic waveguide (Neumann) with a thin slot at the edge. It can be thought as a system coupling the closed thin slot with the trivial semi-infinite waveguide, and, intuitively, it is not surprising that this geometry can posses solution with the wave strongly localized in the slot when the frequency is close to the resonance frequency of the closed slot. The solution plotted in Figure 22 corresponds to such a quasi-trapped wave close to the $\lambda/4$ resonance ($kL \simeq \pi/2$) of the slot. Here, by energy conservation, the reflected power flux is equal to the incident one (and so the wave is leaking towards infinity), but the amplitude in the slot is much larger than in the principal waveguide.

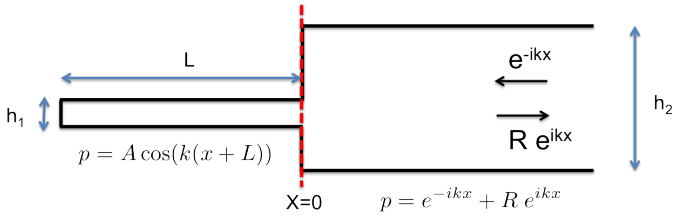

Figure 23. Approximate model for the thin slot quasi-trapping.

To gain further insight, it is useful to look at an approximate solution to this problem. We are at low frequencies so that we can just take the plane wave transverse mode in each part of the waveguide ($kh_2 < \pi$). For $x < 0$, the wave in the slot is given by

$$p = A \cos k(x + L), \tag{39}$$

and in the principal waveguide ($x > 0$):

$$p = e^{-ikx} + Re^{ikx}. \tag{40}$$

The approximate model is summarized in Figure 23. It remains to apply the matching at the interface $x = 0$ that consists in the continuity of p and hp'. These yield the two equations:

$$A\cos(kL) = 1 + R \tag{41}$$

and

$$-Akh_1 \sin(kL) = -ikh_2(1 - R). \tag{42}$$

Eliminating the coefficient A, we find the reflection coefficient R to be

$$R = \frac{1 + i\dfrac{h_1}{h_2}\tan(kL)}{1 - i\dfrac{h_1}{h_2}\tan(kL)}. \tag{43}$$

This simple result is interesting because it illustrates the behavior of a quasi-trapped mode. First, note that $|R| = 1$ for real frequency due to energy conservation. Next, by inspecting what happens for complex k, from (43), it appears that R has pole for k solution of

$$1 - i\frac{h_1}{h_2}\tan(kL) = 0. \tag{44}$$

This complex value of k is the complex resonance frequency (Flax et al., 1981; Aslanyan et al., 2000) corresponding to a quasi-trapped mode. For very thin slot the asymptotic solution of (44) is given by

$$k_R L \simeq \frac{\pi}{2} - i\epsilon \quad (n\pi) \tag{45}$$

where $\epsilon = h_1/h_2 \ll 1$. Hence, we recover the intuitive $\lambda/4$ resonance foreseen in Figure 22, but with an imaginary part due to the leakage of the wave towards infinity.

More generally (independently of the approximate solution presented above), a complex resonance is associated to a mode with complex resonance frequency. It is mode since it is a solution of the homogeneous wave equation with outgoing radiation towards infinity (it can radiate because k has an imaginary part[9]). Thus a complex resonance frequency is both (Aslanyan et al., 2000):

- a complex k for which there is a solution to the homogeneous Helmholtz equation with outgoing radiation condition

[9] This imaginary part has to be negative as will be seen in the next section.

- a complex k that is a pole of the reflection coefficient (or more generally the scattering matrix)

Both definitions are valid because a pole of the reflection coefficient gives a solution to the wave equation without incident wave.

In the time domain, the negative imaginary part of the frequency gives the ringing time of the mode (similar to the radioactive half-life) since with the chosen convention of time dependence $e^{-i\omega t}$ the wave decreases as $e^{\omega_i t}$ where $\omega_i = c\,\mathrm{Imag}(k_R)$. Besides, a complex resonance has a quality factor measuring (as for the harmonic oscillator) how sharp is the resonance. Figure 24 displays a quasi trapped mode for a complex resonance with a very large quality factor. This huge quality factor is due to the weak coupling between the mode of the rectangular cavity and the lead of the waveguide where the the wave can leak.

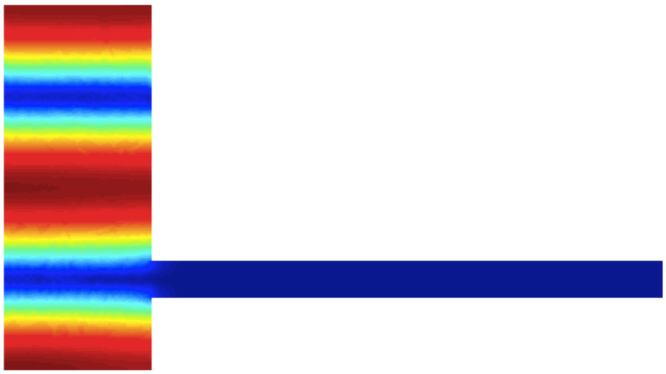

Figure 24. Example of long lived state with quality factor $Q \simeq 10^5$.

4.2 Some properties for complex resonance

It is possible to show that the imaginary part of the complex resonance frequency is positive due to outgoing radiation condition. Let us consider the geometry depicted in Figure 25. A quasi-trapped mode is solution to the wave equation

$$\triangle p + k^2 p = 0, \tag{46}$$

with Neumann boundary condition on the walls and outgoing radiation condition on S_{out}. Multiplying this equation by $\overline{p}$ and integrating on the

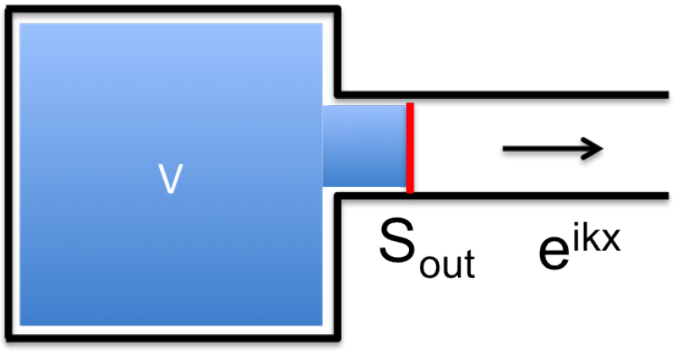

Figure 25. Cavity coupled to a a waveguide.

volume V gives

$$\int_{Sout} \overline{p}\, \partial_n p - \int\int_V |\nabla p|^2 + k^2 \int\int_V |p|^2 = 0. \tag{47}$$

The outgoing radiation condition is translated[10] into $\partial_n p = ikp$ on S_{out} so that we obtain

$$ik \int_{Sout} |p|^2 - \int\int_V |\nabla p|^2 + k^2 \int\int_V |p|^2 = 0. \tag{48}$$

Taking the imaginary part of this equation yields

$$ik_r \int_{Sout} |p|^2 + 2k_i k_r \int\int_V |p|^2 = 0 \tag{49}$$

where k_r and k_i are the real and imaginary part of k. Eventually, it comes that

$$k_i = -\frac{\int_{Sout} |p|^2}{2\int\int_V |p|^2}. \tag{50}$$

Equation (50) demonstrates that the imaginary part of the complex resonance frequency has to be negative. With[11] $k = \omega/c$, we conclude that the

[10] Here, for the sake of simplicity, we assume that only the plane transverse mode has to be taken into account but the exact outgoing radiation condition using the Dirichlet to Neumann operator works similarly.

[11] In this section we are in the dispersionless case where c does not depend on ω so that k and ω are interchangeable.

complex resonance frequency can only be located in the lower half plane $\mathrm{Im}(\omega) < 0$.

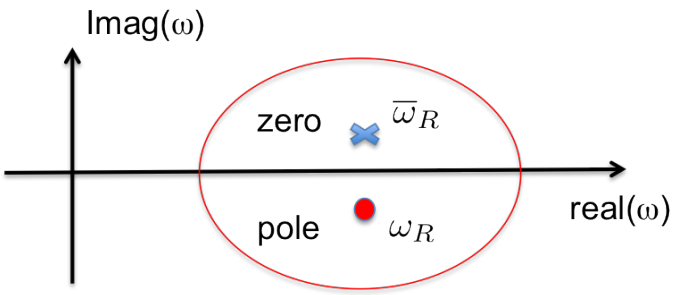

Figure 26. Analytical structure of R in the complex frequency plane.

Besides, by time reversal symmetry (complex conjugation) it appears that[12]

$$\overline{R(\omega)} = \frac{1}{R(\overline{\omega})}. \tag{51}$$

It means that a pole ω_R of the reflection coefficient (complex resonance frequency) is associated to a zero of R at $\overline{\omega}_R$. Locally, near the complex resonance frequency, the reflection coefficient can thus be expressed as

$$R(\omega) = e^{i\theta} \ \frac{\omega - \overline{\omega}_R}{\omega - \omega_R}. \tag{52}$$

The phase θ is slowly varying for ω in the neighborhood of ω_R and it is real for real ω because then $|R| = 1$ by energy conservation. It is termed a background phase term for it represents the slow variation in the scattering compared to the rapid variation due the close resonance frequency ω_R. This local expression for R is very useful: it encodes very simply the local behavior of the quasi-resonance and it explains the universal 2π shift observed for the phase of the scattering. Figure 26 summarizes the analytical structure of the reflection coefficient. Poles (or complex resonance frequency) of R are in the lower half plane and they are mirrored by zeros in the upper half plane.

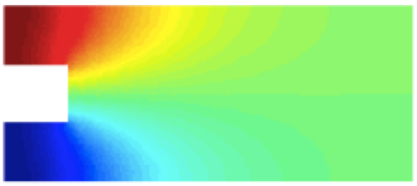

Figure 27. 2D edge resonance in an acoustic waveguide, obtained by symmetry from the trapped mode with a rectangular obstacle.

4.3 Edge waves

A 2D trapped mode in an acoustic waveguide (with Neumann boundary conditions) is solution of the Helmholtz equation

$$(\partial_{xx} + \partial_{yy})\, p + k_R^2 p = 0, \tag{53}$$

with the outgoing boundary condition

$$p(x, y) \to 0 \tag{54}$$

when $x \to 0$. By symmetry w.r.t. the vertical axis, the trapped mode examined in Figure 19 can be converted to a trapped mode in the semi-infinite waveguide shown in Figure 27. This solution is essentially 2D, but what does it imply in 3D?

We consider the extension of the previous geometry to 3D as displayed in Figure 28. An edge wave for the 3D geometry is sought as a solution of the 3D Helmholtz equation

$$(\partial_{xx} + \partial_{yy} + \partial_{zz})\, p + k^2 p = 0 \tag{55}$$

with Neumann boundary conditions at the walls and the outgoing radiation

$$\phi(x, y, z) \to 0 \tag{56}$$

when $x \to 0$. The edge wave propagating along the z axis is written as

$$p(x, y, z) = e^{i\beta z} \phi(x, y). \tag{57}$$

[12] This property is also valid for the scattering matrix (Flax et al., 1981; Aslanyan et al., 2000).

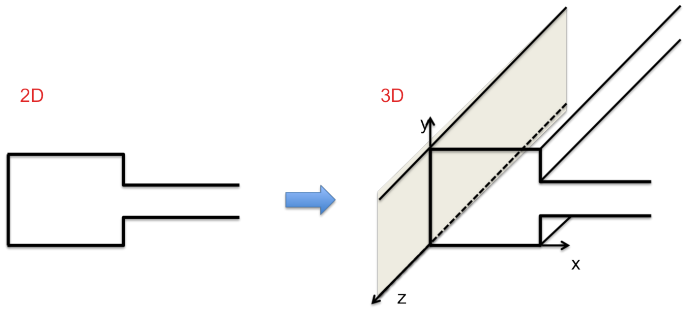

Figure 28. From 2D to 3D.

Inserting Equation (57) into the 3D Helmholtz equation yields the equation for ϕ:

$$(\partial_{xx} + \partial_{yy})\,\phi + (k^2 - \beta^2)\,\phi = 0, \tag{58}$$

with Neumann boundary condition and the condition that $\phi(x, y) \to 0$ when $x \to 0$. The equations and the boundary conditions for ϕ of the 3D edge wave are exactly the same as those of the 2D trapped mode. It means that ϕ is a 2D trapped mode and by comparing Equations (53) and (58):

$$k^2 - \beta^2 = k_R^2. \tag{59}$$

This gives immediately the dispersion relation of the 3D edge wave

$$\frac{\omega^2}{c^2} = \beta^2 + k_R^2. \tag{60}$$

Hence a 2D trapped mode can be converted into a 3D edge wave and the 2D resonance frequency becomes the cut-on frequency in 3D. The corresponding dispersion relation is plotted in Figure 29.

A 2D quasi trapped mode can also be extended to 3D. It is then converted into a 3D leaky edge mode. It is damped (leaky) as it propagates along the z axis since the wave is not perfectly localized at the edge and it radiates continuously some energy. Mathematically, the leakage $\mathrm{Im}(\beta) > 0$ comes from the differentiation of the dispersion relation,

$$\mathrm{Im}(k_R)\mathrm{Re}(k_R) + \mathrm{Im}(\beta)\mathrm{Re}(\beta) = 0,$$

that implies

$$\mathrm{Im}(k_R) < 0 \Rightarrow \mathrm{Im}(\beta) > 0.$$

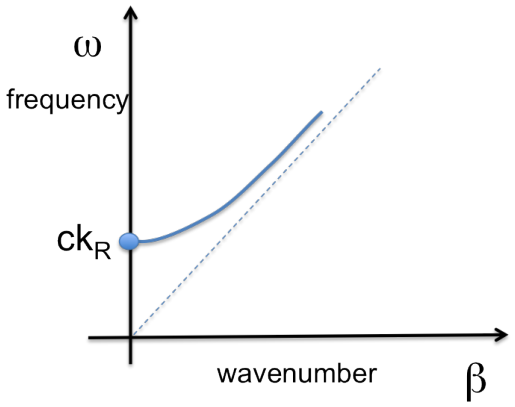

Figure 29. Dispersion relation of the 3D edge wave.

4.4 The simplest edge

Let us examine the simplest case of edge: the semi-infinite strip with a cut at $x = 0$ (Figure 30). Is a trapping of the scalar acoustic wave possible near the edge with a simple boundary condition?

For Dirichlet boundary conditions at the edge $x = 0$,

$$\phi(0, y) = 0$$

automatically results in

$$\phi(x, y) = \sum_n c_n (e^{ik_n x} - e^{-ik_n x}) g_n(y).$$

For Neumann boundary conditions, $\partial_x \phi(0, y) = 0$ imposes

$$\phi(x, y) = \sum_n c_n (e^{ik_n x} + e^{-ik_n x}) g_n(y).$$

We conclude that neither Dirichlet nor Neumann boundary conditions at the edge is able to support an acoustic solution with outgoing boundary conditions towards $x \to \infty$. A richer boundary condition is needed to trap the wave. For scalar waves, impedance at the edge can sustain trapping (but they add a parameter in the problem). In the next section, we will see that elastic waves (vectorial waves) have the ability to trap the wave near the simplest edge with a traction free surface.

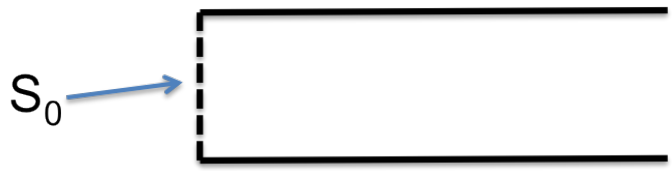

Figure 30. The simplest edge: the semi-infinite strip.

5 Edge resonance in elastic waveguides

5.1 Elastic waveguides

The considered geometry is depicted in Figure 31. The equations of linear elastodynamics for isotropic solid are

$$-\rho\omega^2\mathbf{w} = \nabla.\sigma, \tag{61}$$

where ρ is the mass density, $\mathbf{w} = (u_x, u_y, u_z)^T$ is the elastic displacement and σ is the stress tensor. Owing to the elastic Lamé parameters λ and μ, the Hooke law links the strain tensor to the stress tensor through

$$\sigma = \lambda \, \mathrm{div}\boldsymbol{w} \, \mathrm{Id} + \mu(\nabla\boldsymbol{w} + \nabla\boldsymbol{w}^T). \tag{62}$$

Equation (61) can be be rewritten in term of displacement only:

$$-\rho\omega^2\mathbf{w} = (\lambda + 2\mu)\nabla(\nabla.\mathbf{w}) - \mu\nabla \wedge \nabla \wedge \mathbf{w}. \tag{63}$$

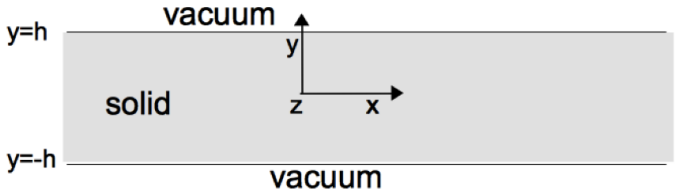

Figure 31. Elastic waveguide.

In free space plane wave solutions can be sought in the form

$$\mathbf{w} = \mathbf{w}_0 \, e^{i\mathbf{kx}}, \tag{64}$$

that makes to appear two different polarizations. The longitudinal wave is such that

$$\mathbf{k} \wedge \mathbf{w}_0 = 0 \tag{65}$$

with a dispersion relation given by

$$k^2 = \frac{\omega^2}{c_L^2} \tag{66}$$

with $c_L^2 \equiv (\lambda + 2\mu)/\rho$. The transversal waves are such that

$$\mathbf{k}.\mathbf{w}_0 = 0 \tag{67}$$

with the dispersion relation

$$k^2 = \frac{\omega^2}{c_T^2} \tag{68}$$

with $c_T^2 = \mu/\rho$. In contrast with acoustic waves (scalar waves), the elastic waves can be called vectorial waves since they have different kinds of polarizations.

In waveguides (Figure 31), the transverse modes are of the form

$$\mathbf{w} = \mathbf{w}_0(y)\, e^{i\mathbf{kx}}, \tag{69}$$

with $\mathbf{k} = q\ \mathbf{e}_x$ and $\partial_z = 0$. Because of the different kinds of polarizations, two families of transverse modes exist:

- SH transverse modes (anti-plane strain). Their non zero components are u_z and (σ_{xz} , σ_{yz}). It corresponds to a scalar wave equivalent to acoustic problem with u_z replacing the pressure and with Neumann boundary conditions at the free stress interface.
- Lamb modes (plane strain). Their non-zero components are (u_x , u_y) and (σ_{xx} , σ_{xy} , σ_{yy} , σ_{zz}). It corresponds to a vectorial wave that is composed of one longitudinal polarization and one transversal polarization.

Having discussed the acoustic case in the previous sections, we now focus on Lamb modes that are vectorial waves. To find the transverse modes it is convenient to write the displacement with two potentials

$$\mathbf{w} = \nabla\phi + \nabla\psi \times e_z, \tag{70}$$

and each of the potentials ϕ and ψ obeys a scalar wave equation

$$(\Delta + k_l^2)\phi = 0 \tag{71}$$

and

$$(\Delta + k_t^2)\psi = 0. \tag{72}$$

The complexity comes from the stress free boundary conditions $\sigma.\mathbf{n} = 0$ with $\mathbf{n} = \pm\mathbf{e}_y$ at $y = \pm h$. They are

$$\sigma_{xy} = (\lambda + 2\mu)\phi_{yy} + \lambda\phi_{xx} - 2\mu\psi_{xy} = 0 \quad \text{at} \quad y = \pm h$$

and

$$\sigma_{yy} = \mu(\psi_{yy} - \psi_{xx} + 2\phi_{xy}) = 0 \quad \text{at} \quad y = \pm h.$$

For transverse modes, the x-dependancies are of the form $f(x, y) = F(y)e^{iqx}$. By using ϕ and ψ that verify (71) and (72) and the boundary conditions, some algebra show that the global dispersion relation can be factorized in two simpler dispersion relations:

$$\frac{\tanh \alpha h}{\tanh \beta h} = \frac{4q^2\alpha\beta}{(q^2 + \alpha^2)^2} \quad \text{for symmetric modes} \tag{73}$$

$$\frac{\tanh \alpha h}{\tanh \beta h} = \frac{(q^2 + \alpha^2)^2}{4q^2\alpha\beta} \quad \text{for antisymmetric modes} \tag{74}$$

with $\alpha = (q^2 - k_t^2)^{1/2}$ and $\beta = (q^2 - k_l^2)^{1/2}$. Symmetric modes have an axial displacement u_x even w.r.t. y whilst antisymmetric modes have u_x odd w.r.t. y.

Each of the dispersion relation 73 and 74 can be written as $D(\Omega, K) = 0$ where $\Omega = k_t h$ is the dimensionless frequency and $K = qh$ is the dimensionless wavenumber. An example of the behavior of the dispersion behavior of Lamb modes is shown in Figures 32 and 33 for an elastic material with Poisson ratio $\nu = 0.3$ ($c_L/c_T \simeq 1.87$). At low frequencies, only modes S_0 and A_0 are propagating; the slope of the curve for S_0 gives the wave speed of longitudinal vibrations in thin plate under the plane stress approximation whilst the parabolic behavior of mode A_0 corresponds to the Kirchhoff equation for thin plate with flexural vibrations. For a given frequency Ω, there is a finite number of propagating modes and an infinity of evanescent modes (with an non-zero imaginary part of the wavenumber, not shown in the Figures). Note the atypical behavior near the cut-on frequency of modes S_1 and S_2 in Figure 32: this pair of modes becomes propagating at points C_1 and C_2 with a non-zero wavenumber K. Moreover, the mode S_2 has a negative phase velocity ($K < 0$) on a narrow band of frequencies.

5.2 Multimodal method in elastic waveguides

It has been remarked that the structure of the Lamb mode spectra is much more complicated than the one of transverse acoustic modes presented

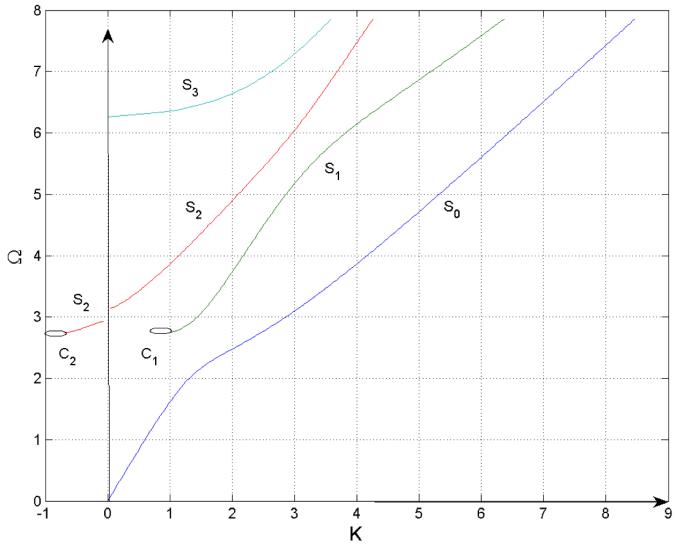

Figure 32. Dispersion diagram of the symmetric Lamb modes.

earlier. In this section, we examine a formalism (Pagneux and Maurel, 2002, 2004, 2006) that facilitates the use of these modes; it make to appear a structure where the projection on the transverse Lamb modes is done using a bi-orthogonality relation.

Elasticity equation can be re-written as

$$\partial_x \begin{pmatrix} \mathbf{X} \\ \mathbf{Y} \end{pmatrix} = \begin{pmatrix} 0 & \mathsf{F} \\ \mathsf{G} & 0 \end{pmatrix} \begin{pmatrix} \mathbf{X} \\ \mathbf{Y} \end{pmatrix}, \tag{75}$$

where vectors $\mathbf{X}$ and $\mathbf{Y}$ are

$$\mathbf{X} = \begin{pmatrix} u_x \\ \sigma_{xy} \end{pmatrix} \quad \text{and} \quad \mathbf{Y} = \begin{pmatrix} -\sigma_{xx} \\ u_y \end{pmatrix},$$

and where F and G are the matrices of differential operators

$$\mathsf{F} = \begin{pmatrix} -\dfrac{f_1}{\lambda} & -f_1\partial_y \\ f_1\partial_y & -\rho\omega^2 - f_2\partial_{y^2} \end{pmatrix}, \quad \text{and} \quad \mathsf{G} = \begin{pmatrix} \rho\omega^2 & \partial_y \\ -\partial_y & \dfrac{1}{\mu} \end{pmatrix}, \tag{76}$$

with $f_1 = \lambda/(\lambda+2\mu)$ and $f_2 = 4\mu(\lambda+\mu)/(\lambda+2\mu)$. The boundary conditions at the stress surfaces, $\sigma.n = 0$ (i.e. $\sigma_{xy} = \sigma_{yy} = 0$ at $y = \pm h$), can be

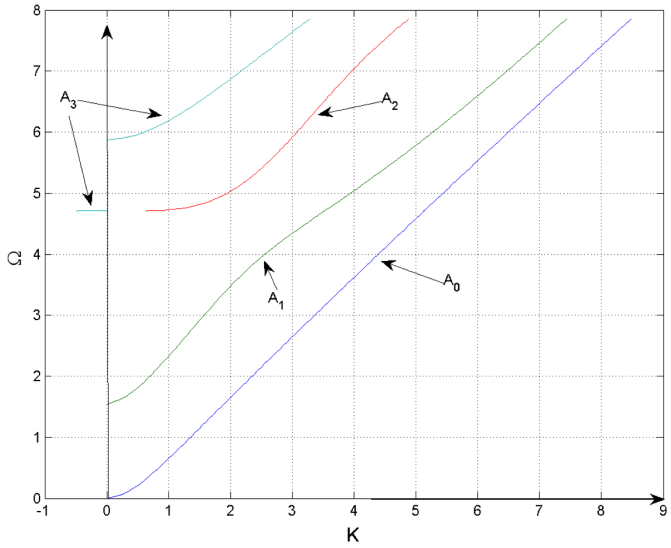

Figure 33. Dispersion diagram of the antisymmetric Lamb modes.

expressed directly on components $\mathbf{X}$ and $\mathbf{Y}$ for σ_{xy} is the second component of $\mathbf{X}$ and $\sigma_{yy} : \mathbf{Y} \to \sigma_{yy}(\mathbf{Y}) = f_1\sigma_{xx} + f_2\partial_y u_y$.

The equation to find the transverse Lamb modes takes the explicit form (the x dependance e^{iqx} implies that ∂_x becomes iq) of an eigenvalue problem

$$iq \begin{pmatrix} \mathbf{X} \\ \mathbf{Y} \end{pmatrix} = \begin{pmatrix} 0 & \mathsf{F} \\ \mathsf{G} & 0 \end{pmatrix} \begin{pmatrix} \mathbf{X} \\ \mathbf{Y} \end{pmatrix}, \tag{77}$$

and the boundary conditions (i.e. $\sigma_{xy} = \sigma_{yy} = 0$ at $y = \pm h$) does not involve the eigenvalue q. Lamb modes are thus eigenvectors of this eigenproblem with eigenvalues q. There is an infinity of modes: right-going transverse modes have eigenvalues q_n and eigenvectors $[\mathbf{X}_n, \mathbf{Y}_n]^T$ and left-going transverse modes have eigenvalues $-q_n$ and eigenvectors $[-\mathbf{X}_n, \mathbf{Y}_n]^T$. Assuming the completeness of Lamb modes, any solution can be expanded as

$$\begin{pmatrix} \mathbf{X} \\ \mathbf{Y} \end{pmatrix} = \sum_{n\geq 0} a_n^+ \begin{pmatrix} \mathbf{X}_n \\ \mathbf{Y}_n \end{pmatrix} + \sum_{n\geq 0} a_n^- \begin{pmatrix} -\mathbf{X}_n \\ \mathbf{Y}_n \end{pmatrix}. \tag{78}$$

The terms of the series can be rearranged to give

$$\mathbf{X} = \sum_{n\geq 0} a_n \mathbf{X}_n \tag{79}$$

and

$$\mathbf{Y} = \sum_{n\geq 0} b_n \mathbf{Y}_n \tag{80}$$

with

$$a_n = a_n^+ - a_n^-$$

and

$$b_n = a_n^+ + a_n^-.$$

Note that the sum are restricted to positive index numbers.

The operators F and G have a very nice property:

$$\begin{array}{ll} (\mathsf{F}\tilde{\mathbf{Y}}|\mathbf{Y}) & = (\tilde{\mathbf{Y}}|\mathsf{F}\mathbf{Y}) + [\sigma_{yy}\tilde{u}_y - \tilde{\sigma}_{yy}u_y]_{-h}^{h} \\ (\mathsf{G}\tilde{\mathbf{X}}|\mathbf{X}) & = (\tilde{\mathbf{X}}|\mathsf{G}\mathbf{X}) + [u_x\tilde{\sigma}_{xy} - \tilde{u}_x\sigma_{xy}]_{-h}^{h}. \end{array} \tag{81}$$

Hence, F and G are symmetric with the inner product defined by[13]

$$\left(\begin{pmatrix} u_1 \\ v_1 \end{pmatrix} | \begin{pmatrix} u_2 \\ v_2 \end{pmatrix}\right) = \int_{-h}^{h} (u_1u_2 + v_1v_2)dy$$

for the elastic waves with stress free boundary conditions at $y = \pm h$ since $\sigma_{xy}(\pm h) = 0$ and $\sigma_{yy}(\pm h) = 0$, see (81). It is then easy to show that $(k_m^2 - k_n^2)(\mathbf{X}_m|\mathbf{Y}_n) = 0$ for two Lamb modes with indices m and n. The chosen formalism and the properties of F and G allow to directly prove the bi-orthogonality condition:

$$(\mathbf{X}_n|\mathbf{Y}_m) = J_n\delta_{mn}. \tag{82}$$

Eventually, the projections on the Lamb modes are made easy: from the equations (79) and (80), the components a_n and b_n are given by

$$(\mathbf{Y}_n|\mathbf{X}) = J_n a_n$$

and

$$(\mathbf{X}_n|\mathbf{Y}) = J_n b_n.$$

5.3 2D edge resonance

Let us consider a very simple configuration: a 2D semi infinite elastic waveguide of width h embedded in vacuum. The edge is at $x = 0$ and the guide is in the $(x > 0, -h < y < h)$ region (geometry of Figure 34). If the

[13] This inner product is not a scalar product because the vectors $\mathbf{X}$ and $\mathbf{Y}$ are complex.

wave is excited at $x = 0$ by a source imposing $\mathbf{X}(x = 0, y)$ or $\mathbf{Y}(x = 0, y)$, the solution has only right-going wave and can be expressed as

$$\begin{cases} \mathbf{X} = \sum_{n\geq 0} \alpha_n e^{iq_n x} \mathbf{X}_n(y), \\ \mathbf{Y} = \sum_{n\geq 0} \alpha_n e^{iq_n x} \mathbf{Y}_n(y), \end{cases} \tag{83}$$

because $a_n^- = 0$. The coefficients α_n are uniquely determined by the bi-orthogonality relation (82)

$$(\mathbf{X}(x = 0, y)|\mathbf{Y}_n) = J_n \alpha_n \quad \text{or} \quad (\mathbf{Y}(x = 0, y)|\mathbf{X}_n) = J_n \alpha_n.$$

That means that, for this problem posed with an initial condition on $\mathbf{X}$ or $\mathbf{Y}$ (a mixed condition since it is concerned with one component of displacement and one component of the stress tensor), we have the uniqueness of the solution: the solution is zero for $\mathbf{X}(x = 0, y) = 0$ or $\mathbf{Y}(x = 0, y) = 0$.

What happens now if the the constraint $\sigma.n$ is imposed as a source at $x = 0$? It gives the values of σ_{xx} and σ_{xy} which corresponds to one component of $\mathbf{X}$ and one component of $\mathbf{Y}$. Thus, to impose the constraint $\sigma.n$ at $x = 0$ is a mixed condition in the $\mathbf{XY}$ formalism, and the bi-orthogonality relation does not allow the projection of the solution on the Lamb modes: it seems that uniqueness is not ensured. Said differently, if $\sigma_{xx} = 0$ and $\sigma_{xy} = 0$ are imposed at $x = 0$, it is possible to have a non-zero solution with outgoing radiation condition in the very simple problem of the semi-infinite elastic waveguide. This solution corresponds to a localized mode of vibration, trapped on the free edge at $x = 0$.

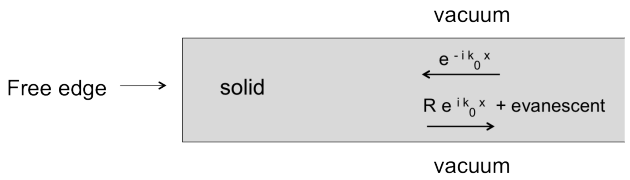

Figure 34. Reflection of the S_0 Lamb mode by a free edge.

The linear elastic equation can be written in a dimensionless from by normalizing all the lengths by the semi-width h and the stress by the Lamé coefficient μ:

$$\partial_x \begin{pmatrix} \mathbf{X} \\ \mathbf{Y} \end{pmatrix} = \begin{pmatrix} 0 & F \\ G & 0 \end{pmatrix} \begin{pmatrix} \mathbf{X} \\ \mathbf{Y} \end{pmatrix}, \tag{84}$$

with

$$F = \frac{1}{\gamma}\begin{pmatrix} -1 & -(\gamma-2)\partial_y \\ (\gamma-2)\partial_y & -\gamma\Omega^2 - 4(\gamma-1)\partial_{y^2} \end{pmatrix} \tag{85}$$

and

$$G = \begin{pmatrix} \Omega^2 & \partial_y \\ -\partial_y & 1 \end{pmatrix}, \tag{86}$$

with $\gamma = (\lambda + 2\mu)/\mu = c_L^2/c_T^2$. The boundary conditions $\sigma.n = 0$ at the traction free surfaces are

$$\begin{cases} \sigma_{xy} = 0 \\ \sigma_{yy} = 1/\gamma((\gamma-2)\sigma_{xx} + 4(\gamma-1)\partial_y u_y) = 0 \end{cases} \quad \text{at} \quad y = \pm 1, \tag{87}$$

on the horizontal faces and

$$\begin{cases} \sigma_{xy} = 0 \\ \sigma_{xx} = 0 \end{cases} \quad \text{at} \quad x = 0. \tag{88}$$

Since $\gamma = 2(1-\nu)/(1-2\nu)$ ($0 < \nu < 1/2$ is the Poisson ratio) and $\Omega = k_T h$, when made dimensionless, the problem of vibrations of the semi-infinite elastic waveguide *depends only on two parameters*: the frequency Ω and the Poisson ratio ν.

In the following we will consider only symmetric waves (with Lamb modes S_n) for frequency below the cut-on frequency of the mode S_1 (see points C_1 and C_2 in Figure 32): only the mode S_0 is propagating. To study the edge resonance it is convenient to pose the problem as a reflection problem. The situation is described in Figure 34 with a left-going S_0 incident wave and a reflected right-going field composed of the propagating S_0 (with reflection coefficient R) and the remaining evanescent Lamb modes $(S_1, S_2, S_3, ...)$. The solution can be written as[14]

$$\begin{pmatrix} \mathbf{X} \\ \mathbf{Y} \end{pmatrix} = e^{-ik_0 x}\begin{pmatrix} \mathbf{X}_0 \\ -\mathbf{Y}_0 \end{pmatrix} + Re^{ik_0 x}\begin{pmatrix} \mathbf{X}_0 \\ \mathbf{Y}_0 \end{pmatrix} + \sum_{n=1}^{+\infty} a_n e^{ik_n x}\begin{pmatrix} \mathbf{X}_n \\ \mathbf{Y}_n \end{pmatrix}. \tag{89}$$

For real frequency Ω, the conservation of energy imposes that $|R| = 1$. Several authors have studied that reflection coefficient (Shaw, 1956; Torvik, 1967; Auld and Tsao, 1977; M. Koshiba et al., 1983; Gregory and Gladwell, 1983; Le Clezio et al., 2003) and they all showed the same behavior of R as a function of the real frequency. Figure 35 displays this behavior for a

[14] In contrast to the previous section, the convention here is $\mathbf{X}_0^- = \mathbf{X}_0^+$ and $\mathbf{Y}_0^- = -\mathbf{Y}_0^+$ in order to have a reflection coefficient R tending to 1 at low frequencies.

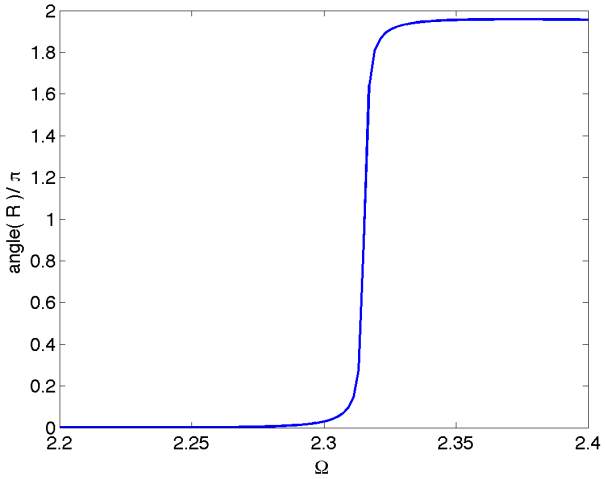

Figure 35. Phase of the reflection coefficient R as a function of frequency for $\nu = 0.3$.

Poisson ratio $\nu = 0.3$: the phase of R has a rapid variation of the phase near a particular frequency. This is the typical behavior of a quasi-trapped mode, i.e. a complex resonance frequency that has a finite quality factor in the harmonic regime (Ω real). By using the variational tools of functional analysis, Roitberg et al. (1998) have proved that a trapped mode exists for this free edge. The works in Zernov et al. (2006) and Pagneux (2006) have shown that, in fact, there is one complex resonance frequency Ω_R for each value of the Poisson ratio ν.

The complex resonance frequency Ω_R is written as

$$\Omega_R(\nu) = \Omega'_R(\nu) + i\Omega"_R(\nu)$$

which corresponds to a quality factor $Q = \Omega'_R/(2|\Omega"_R|)$. As seen in section 4, a complex resonance frequency is associated to a quasi-trapping without incident mode and it is also a pole of the reflection coefficient R with $\mathrm{Im}(\Omega) < 0$. The edge resonance frequency $\Omega_R(\nu)$ corresponds to a pole of $R(\Omega, \nu)$.

Figures 36 and 37 show the behavior of Ω_R as a function of the Poisson ratio. The real part is monotone and it corresponds to the value of the frequency of quasi-resonance in the harmonic regime (cf. Figure 36). A

very accurate empirical expression (Pagneux, 2006) for this real part is

$$\mathrm{Re}(\Omega_R) = 0.652\nu^2 + 0.898\nu + 1.9866$$

whose error is less than 10^{-3}.

The imaginary part of the complex resonance frequency has a more complicated behavior: Figure 28, which shows $-\Omega"_R$ on a logarithmic scale, demonstrates that there are two values of the Poisson ratio where the quasi-trapped mode becomes a perfectly trapped mode with a real resonance frequency. The perfect resonance at $\nu = 0$ is due to a particular symmetry of the elasticity equation discovered by Roitberg et al. (1998). They showed that, for $\nu = 0$ (i.e. $\lambda = 0$), the elastic field can be decomposed into two parts that are decoupled:

$$\begin{pmatrix} u_x \\ u_y \end{pmatrix} = \begin{pmatrix} \frac{1}{2h}\int_{-h}^{h} u_x dy \\ 0 \end{pmatrix} + \begin{pmatrix} u_x - \frac{1}{2h}\int_{-h}^{h} u_x dy \\ u_y \end{pmatrix}. \tag{90}$$

The first part contains the propagating S_0 mode and the second part all the remaining evanescent waves. This subtle decoupling is similar to the simpler one that was presented for trapped modes in Neumann waveguides in section 3, and it allows the trapped mode at the real Ω_R that does not radiate through the propagating S_0 Lamb mode. The other perfect resonance at $\nu = 0.2248$ can be explained by the uncoupled reflection of the Lamé mode (Pagneux, 2006). Note the low values of $\mathrm{Im}(\Omega_R)$ that imply that the edge resonance has a large quality factor.

5.4 Edge resonance for cylinders

The edge resonance exists also for semi-infinite cylinders with traction free boundary conditions (Gregory and Gladwell, 1989; Holst and Vassiliev, 2000; Pagneux, 2012). The problem under study corresponds to the semi-infinite circular rod geometry with the vertical edge at $z = 0$ and the horizontal surfaces at $r = a$, where (r, θ, z) are the cylindrical coordinates. The domain of the solid rod is defined by $r < a$ and $z > 0$.

We consider elastic waves that are axially symmetric with displacement components in the radial and axial directions (Zemanek, 1972; Graff, 1991): $\mathbf{w} = (u_r(r,z), 0, u_z(r,z))^T$. By taking into account these symmetries and by making dimensionless the equations (renormalizing all the lengths by a and the stress tensor by μ), the equations become

$$\begin{aligned} -\Omega^2 u_r &= \partial_r \sigma_{rr} + \partial_z \sigma_{rz} + \frac{\sigma_{rr} - \sigma_{\theta\theta}}{r}, \\ -\Omega^2 u_z &= \partial_r \sigma_{rz} + \partial_z \sigma_{zz} + \frac{\sigma_{rz}}{r}, \end{aligned} \tag{91}$$

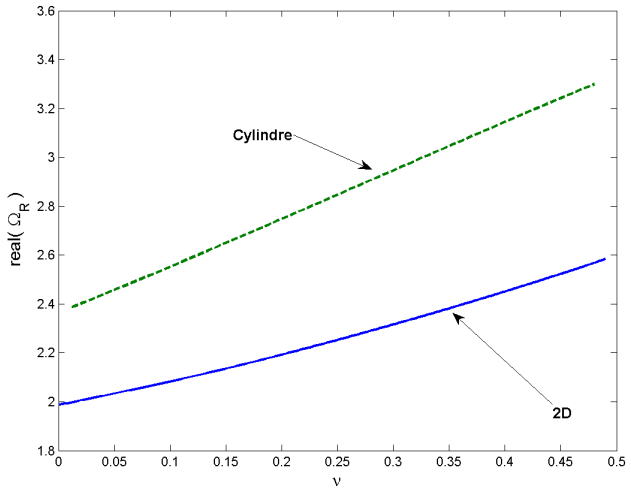

Figure 36. Real part of the complex resonance frequency.

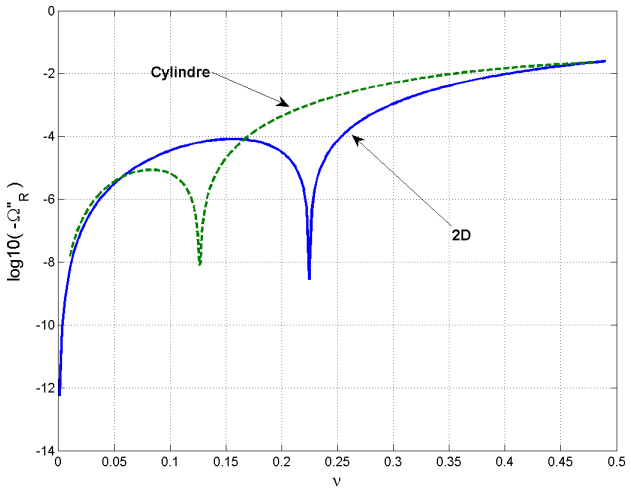

Figure 37. Imaginary part of the complex resonance frequency.

$$\begin{aligned}
\sigma_{rr} &= 2\partial_r u_r + (\gamma-2)(\frac{1}{r}\partial_r(ru_r) + \partial_z u_z),\\
\sigma_{\theta\theta} &= 2\frac{u_r}{r} + (\gamma-2)(\frac{1}{r}\partial_r(ru_r) + \partial_z u_z),\\
\sigma_{zz} &= 2\partial_z u_z + (\gamma-2)(\frac{1}{r}\partial_r(ru_r) + \partial_z u_z),\\
\sigma_{rz} &= \partial_z u_r + \partial_r u_z,
\end{aligned} \tag{92}$$

with the frequency $\Omega = \omega a/c_T$. It is similar to the one defined in 2D with the 2D semi-height h replaced by the radius a.

The stress free boundary conditions at the horizontal surface ($r = 1$) and at the free edge ($z = 0$) are

$$\begin{aligned}
&\sigma_{rr} = \sigma_{rz} = 0 \quad \text{at } r = 1,\\
&\sigma_{zz} = \sigma_{rz} = 0 \quad \text{at } z = 0.
\end{aligned} \tag{93}$$

Note that, as in 2D, there are only two parameters: the frequency Ω and the Poisson ratio ν.

In this axisymmetric geometry the Lamb modes are replaced by the Pochhammer modes (Graff, 1991) whose dispersion relation is

$$(-k^2 + b^2)^2 J_0(d)J_1(b) + 4bdk^2 J_0(b)J_1(d) - 2d\Omega^2 J_1(d)J_1(b) = 0$$

with $b = \sqrt{\Omega^2 - k^2}$ and $d = \sqrt{\Omega^2/\gamma - k^2}$. We will consider frequency Ω such that only the first mode, $n = 0$, is a propagating mode and it will be called the L_0 mode. All the other modes, L_n with $n \geq 1$, are evanescent with $\mathrm{Im}(k_n) > 0$.

As in 2D, there is one complex resonance frequency Ω_R for each value of the Poisson ratio ν. The real value of Ω_R is displayed in Figure 36. The quasi-linear behavior as a function of ν is very well approximated (Pagneux, 2012) by the empirical formula

$$\mathrm{Re}(\Omega_R) = 1.9624\nu + 2.3573,$$

accurate up to 0.3%. Figure 37 shows the behavior of the imaginary part of Ω_R. Once again, as in 2D, there are two values of the Poisson ratio where the trapping is perfect with a zero imaginary part of Ω_R and no radiation from the edge. The first value ($\nu = 0$) was discovered by Holst and Vassiliev (2000) by the use of a symmetry similar the one of equation (90) and the second value ($\nu = 0.1267$) was found in Pagneux (2012) and it is linked to the Lamé mode. The shape of the localized vibration is shown if FIgure 38.

5.5 Edge resonance in 3D plate

The study of the 2D elastic edge resonance has been extended to 3D in Zernov and Kaplunov (2008). These authors have shown that along the

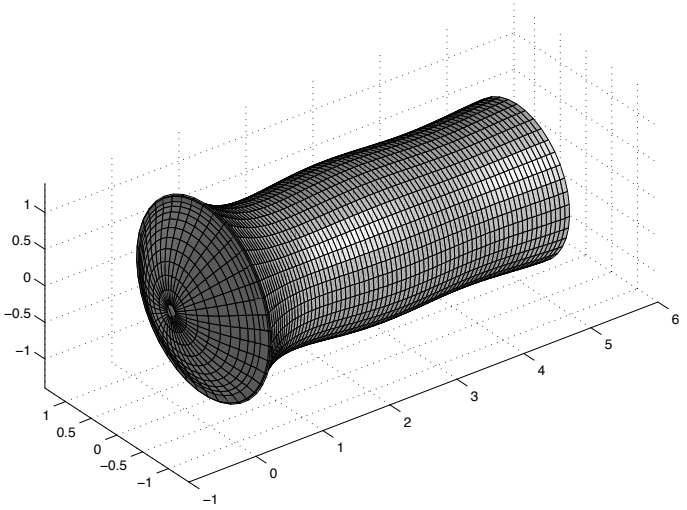

Figure 38. Shape of the localized vibration at edge resonance for $\nu = 0.3$.

stress free straight edge there are two edge waves: the first one has no cut-on frequency and is similar to a generalized Rayleigh wave, the second one is the 3D counterpart of the 2D edge resonance we have considered before with Ω_R playing the role of the cut-on frequency.

Another 3D plate configuration is the one depicted in Figure 39. In this case, it can be shown (Pagneux and Clorennec, 2012) that there exists also a edge resonance for axisymmetric vibration around the hole.

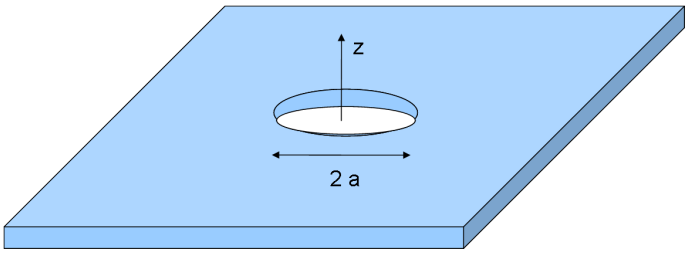

Figure 39. Hole in a 3D plate.

5.6 Concluding remarks

In these notes, we looked at the perfectly localized trapped modes and the ubiquitous slightly radiating quasi-trapped modes. In practice, the difference between these two families of modes is not so clear since, in an experiment, the inevitable attenuation prevents an infinite quality factor (i.e. a perfect resonance). It remains that the study of trapped modes provides clues to efficient resonance mechanisms. The specific ability of trapping for elastic waves near surface with traction-free boundary condition has also been discussed. The well known Rayleigh surface wave already testifies to this ability. Few examples in elastic waveguides have been examined in this chapter and the conclusion might be that we have to mind the edge effects in elastodynamics.

Bibliography

A. Aslanyan, L. Parnovski and D. Vassiliev. Complex Resonances In Acoustic Waveguides. *Quarterly J. Mechanics Applied Mathematics*, 53: 429–447, 2000.

A. Auld and E. M. Tsao. A variational analysis of edge resonance in a semi-infinite plate. *IEEE Trans. Sonics Ultrason.*, 24: 317–326, 1977.

A.S. Bonnet-BenDhia and F. Mahé. A guided mode in the range of the radiation modes for a rib waveguide. *J. Optics*, 28: 4143, 1997.

A.S. Bonnet-BenDhia and J.F. Mercier. Resonances of an elastic plate in a compressible confined fluid. *Quarterly Journal of Mechanics and Applied Mathematics*, 60: 397–421, 2007.

M. Callan, C. M. Linton and D. V. Evans. Trapped modes in two-dimensional waveguides. *J. Fluid Mech.*, 229: 51-64, 1991.

P. Cobelli, V. Pagneux, A. Maurel and P. Petitjeans. Experimental study on water wave trapped modes. *J. Fluid Mech.*, 666: 445–476, 2011.

P. Duclos and P. Exner. Curvature-induced bound states in quantum waveguides in two and three dimensions. *Rev. Math. Phys.*, 7: 73–102, 1995.

D.V. Evans, M. Levitin, and D. Vassiliev. Existence theorems for trapped modes. *J. Fluid Mech.*. 26: 21-31, 1994.

L. Flax, G.C. Gaunaurd and H. berall. Theory of resonance scattering. *Physical Acoustics*, Volume 15, pages 191-294, 1981.

K.F. Graff. *Wave Motion in Elastic Solids*, Dover, 1991.

E. Granot. Emergence of a confined state in a weakly bent wire. *Phys. Rev. B*, 65: 233101, 2002.

R. D. Gregory and I. Gladwell. The reflection of a symmetric Rayleigh-Lamb wave at the fixed or free edge of a plate. *J. Elast.*, 13: 185–206, 1983.

R.D. Gregory and I. Gladwell. Axisymmetric waves in a semi-infinite elastic rod. *Q. J. Mech. Appl. Math.*, 42: 327–337, 1989.

A. Holst and D. Vassiliev. Edge resonance in an elastic semi-infinite cylinder. *Applicable Anal.*, 74: 479–495, 2000.

D. S. Jones. The eigenvalues of $\nabla^2 u + \lambda u = 0$ when the boundary conditions are given in semi-infinite domains. *Proc. Camb. Phil. Soc.*, 49: 668–684, 1953.

J. D. Kaplunov and S.V. Sorokin. A simple example of a trapped mode in an unbounded waveguide. *J. Acoust. Soc. Am.*, 97: 3898, 1995.

M. Koshiba, S. Karakida, and M. Suzuki. Finite-element analysis of edge resonance in a semi-infinite plate. *Electron. Lett.*, 19: 256–257, 1983.

L. D. Landau and E. M. Lifshitz. *Quantum Mechanics: Nonrelativistic Theory*, Pergamon Press, 1977

E. Le Clezio, M. V. Predoi, M. Castaings, B. Hosten, and M. Rousseau. Numerical predictions and experiments on the free-plate edge mode, *Ultrasonics*, 41: 25–40, 2003.

C.M. Linton and P. McIver. Embedded trapped modes in water waves and acoustics. *Wave Motion*, 45: 16-29, 2007.

M. McIver, C.M. Linton, P. McIver, J. Zhang and R. Porter. Embedded trapped modes for obstacles in two-dimensional waveguides. *Quarterly J. Mechanics Applied Mathematics*, 54: 273–293, 2001.

P. M. Morse and K, U. Ingard. *Theoretical Acoustics*, McGraw Hill, New York, 1968.

S.A. Nazarov. Asymptotic expansions of eigenvalues in the continuous spectrum of a regularly perturbed quantum waveguide *Theoretical and mathematical physics*, 167: 606–627, 2011.

V. Pagneux and A. Maurel. Lamb wave propagation in inhomogeneous elastic waveguides. *Proc. R. Soc. London, Ser. A*, 458: 19131930, 2002.

V. Pagneux and A. Maurel. Scattering matrix properties with evanescent modes for waveguides in fluids and solids. *J. Acoust. Soc. Am.*, 116: 1913–1920, 2004.

V. Pagneux and A. Maurel. Lamb wave propagation in elastic waveguides with variable thickness. *Proc R Soc Lond A*, 462: 1315–1339, 2006.

V. Pagneux. Revisiting the edge resonance for Lamb waves in a semi-infinite plate. *J. Acoust. Soc. Am.*,120: 649–656, 2006.

V. Pagneux. Complex resonance and localized vibrations at the edge of a semi-infinite elastic cylinder. *Mathematics and Mechanics of Solids*, 17: 17–26, 2012.

V. Pagneux and D. Clorennec. Complex edge resonance around a hole in a 3D plate. *to be submitted*, 2012.

J. Postnova and R.V. Craster. Trapped modes in elastic plates, ocean and quantum waveguides. *Wave Motion*, 45: 565-579, 2008.

I. Roitberg, D. Vassiliev, and T. Weidl. Edge resonance in an elastic semi-strip. *Q. J. Mech. Appl. Math.*, 51: 1–13, 1998.

E. A. G. Shaw. On the resonant vibrations of thick barium titanate disks. *J. Acoust. Soc. Am.*, 28: 38–50, 1956.

I. Stakgold. *Green's Functions and Boundary Value Problems*, Wiley Interscience, 1998.

P. J. Torvik. Reflection of wave trains in semi-infinite plates. *J. Acoust. Soc. Am.*, 41: 346–353,1967.

J. Zemanek. An experimental and theoretical investigation of elastic wave propagation in a cylinder. *J. Acoust. Soc. Am.*, 51: 265–283, 1972.

V. Zernov, A.V. Pichugin and J. Kaplunov. Eigenvalue of a semi-infinite elastic strip. *Proc. R. Soc. Lond. A*, 462: 1255–1270, 2006.

V. Zernov and J. Kaplunov. Three-dimensional edge waves in plates. *Proc. R. Soc. Lond. A*, 464: 301–318, 2008.